

Joys and Pitfalls of Fermi Surface Mapping in $\text{Bi}_2\text{Sr}_2\text{CaCu}_2\text{O}_{8+\delta}$ Using Angle Resolved Photoemission

S. V. Borisenko,* M. S. Golden, S. Legner, T. Pichler, C. Dürr, M. Knupfer, and J. Fink
Institut für Festkörper- und Werkstofforschung Dresden, P.O. Box 270016, D-01171 Dresden, Germany

G. Yang and S. Abell
School of Metallurgy and Materials, The University of Birmingham, Birmingham, B15 2TT, United Kingdom

H. Berger
Institut de Physique Appliquée, Ecole Polytechnique Fédérale de Lausanne, CH-1015 Lausanne, Switzerland
 (Received 15 December 1999)

On the basis of angle-scanned photoemission data recorded using *unpolarized* radiation, with high (E, \mathbf{k}) resolution, and an extremely dense sampling of \mathbf{k} space, we resolve the current controversy regarding the normal state Fermi surface (FS) in $\text{Bi}_2\text{Sr}_2\text{CaCu}_2\text{O}_{8+\delta}$. The true picture is simple, self-consistent, and robust: the FS is holelike, with the form of rounded tubes centered on the corners of the Brillouin zone. Two further types of features are also clearly observed: shadow FSs, which are most likely to be due to short range antiferromagnetic spin correlations, and diffraction replicas of the main FS caused by passage of the photoelectrons through the modulated Bi-O planes.

PACS numbers: 74.25.Jb, 71.18.+y, 74.72.Hs, 79.60.-i

The topology and character of the normal state Fermi surfaces (FSs) of the high temperature superconductors have been the object of both intensive study and equally lively debate for almost a decade. Angle resolved photoemission spectroscopy (ARPES) has played a defining role in this discussion. In particular, the pioneering work of Aebi *et al.* illustrated that angle-scanned photoemission using unpolarized radiation can deliver a direct, unbiased image of the complete FS of $\text{Bi}_2\text{Sr}_2\text{CaCu}_2\text{O}_{8+\delta}$ (Bi2212) [1], confirming the large FS centered at the corners of the Brillouin zone predicted by band structure calculations [2]. Furthermore, the use of the mapping method enabled the identification of weak additional features (dubbed the shadow Fermi surface or SFS) which were attributed to the effects of short range antiferromagnetic spin correlations, the existence of which had already been proposed theoretically [3]. Subsequently, conventional ARPES investigations [involving the analysis of a series of energy distribution curves (EDCs) along a particular line in \mathbf{k} -space] clearly identified a further set of dispersive photoemission structures which are extrinsic and result from a diffraction of the outgoing photoelectrons as they pass through the structurally modulated Bi-O layer, which forms the cleavage surface in these systems [4].

Recently, this whole picture of the normal state FS of Bi2212 has been called into question. ARPES data recorded using particular photon energies (32–33 eV) have been interpreted in terms of a FS with missing segments [5], an extra set of one-dimensional states [6], or an electronlike FS centered around the Γ point [7]. A further study suggests that both electronlike or holelike FS pieces can be observed merely depending on the photon energy used in the ARPES experiment [8].

These points illustrate that the situation with regard to the true topology and character of the normal state FS of Bi2212 as seen by photoemission spectroscopy is, in fact, far from clear. Thus, considering both the fundamental significance of the FS question in general and the importance of photoemission in this debate, it is essential that an unambiguous framework is arrived at for the interpretation of the ARPES data.

In this Letter we present angle-scanned photoemission data from pure and Pb-doped Bi2212. As our data sets contain more than 1000 high (E, \mathbf{k})-resolved EDCs per Brillouin zone quadrant, we combine the advantages of both the mapping and the EDC methods, making data manipulation such as interpolation superfluous. We show that the origin of the recent controversy stems from the simultaneous presence of three different types of photoemission features around the \bar{M} point [9]: the main FS, diffraction replicas (DRs) and the SFS.

The ARPES experiments were performed using monochromated, unpolarized He I radiation and a SCIENTA SES200 analyzer, enabling simultaneous analysis of both the E and \mathbf{k} distribution of the photoelectrons. The overall energy resolution was set to 30 meV and the angular resolution to $\pm 0.38^\circ$, which gives $\Delta \mathbf{k} \leq 0.028 \text{ \AA}^{-1}$ (i.e., 2.4% of ΓX). High quality single crystals of pristine [10] and Pb-doped Bi2212, the latter grown from the flux in the standard manner, were cleaved *in situ* to give mirror-like surfaces, and all data were measured at either 120 or 300 K within 6 h of cleavage.

Figures 1a and 1b show a series of photoemission data ($T \sim 300 \text{ K}$) of Bi2212 taken along the two high symmetry directions ΓX and ΓY in \mathbf{k} space [9], respectively. The EDCs (right panels) are shown together with 2D (E, \mathbf{k})

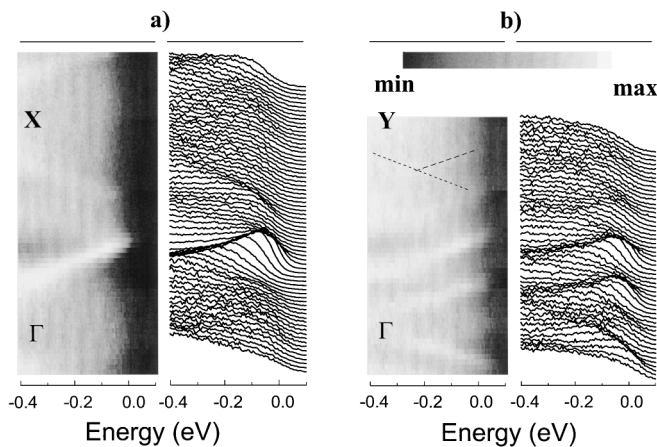


FIG. 1. ARPES of Bi2212 recorded at 300 K along (a) ΓX and (b) ΓY . In each case, the right panels show the EDCs and the left panels show (E, \mathbf{k}) plots in which the photoemission intensity is represented by the grey scale.

representations where the photoemission intensity [11] forms the grey scale (left panels).

We deal first with ΓX . Starting from the Γ point, we clearly observe the main CuO_2 derived band crossing the Fermi level, E_F , at $\sim 0.4(\pi, -\pi)$. Also evident are two weaker features straddling the X point, which cross E_F at wave vectors equivalent to the main band crossings but shifted by the vector $(\pi, -\pi)$. These are the shadow bands first observed in Ref. [1]. A strikingly different picture occurs for ΓY [parallel to the crystallographic b axis (Fig. 1b)]. Once again, the strongest feature is the main band, but now additional, extrinsic DRs of the main band are clearly visible, shifted in \mathbf{k} from the main band by $n\mathbf{q} = (0.21\pi, 0.21\pi)$, whereby n is the order of the DR [4]. Thus, starting from the bottom of Fig. 1b, we see firstly a first-order DR of the main band [the latter crosses E_F at $\sim 0.4(-\pi, -\pi)$]. Then, near the Γ point a feature resulting from the overlap of very weak second-order DRs is observed. There then follows a first-order DR of the parent main band which is then itself seen crossing E_F at $\sim 0.4(\pi, \pi)$. Subsequently, a further first-order DR of the same main band is seen, followed by indications for the shadow band and a second-order DR. It should be stressed that the strongly dispersive nature of the states along $\Gamma X, Y$ eases the task of interpreting the photoemission data.

Thus, the data shown in Fig. 1 indicate the presence of three different types of features for the $\Gamma X, Y$ photoemission data from Bi2212 related to the main bands, the shadow bands, and diffraction replicas of the main bands. In this point there is a broad consensus [1,4,7].

The picture for the region around the \bar{M} point, however, is currently the subject of considerable controversy. In fact, the interpretation of the photoemission data from this region of \mathbf{k} space is the key to resolving this debate and settling, once and for all, the true FS nature and topology in Bi2212.

Therefore, in Fig. 2 we present a detailed momentum map of the normal state ($T = 120$ K) Fermi surface of Bi2212 around the \bar{M} point. The image is based upon 1300 EDCs [11], each of energy width $500 \leq E_B \leq -100$ meV, and thus combines the unbiased view given by a map with the security of being able to examine a full EDC at each particular \mathbf{k} point. Following the discussion of Fig. 1, we have added guidelines indicating the location of the main FS (thick black solid line), the DRs [first order: thin black solid line (on top of the map); second order: dashed black line], and the shadow features (thick red solid line).

The main FS appears in Fig. 2 as arcs of high intensity centered around the X and Y points. There is absolutely no indication of a “closure” of the two main FS arcs shown in Fig. 2 at $(0.8\pi, 0)$ as reported in Refs. [7,8]. Thus there is no Γ -centered (electronlike) FS. The diffraction replicas of the main FS are also clearly present, both individually [e.g., the sole (red) feature on the dark blue background along the Γ - \bar{M} - Z direction at $(1.5\pi, 0)$ is a first-order DR] and collectively (in principle up to infinite order), leading to a bundling of intensity along a ribbon centered on the $(0, -\pi)$ - $(\pi, 0)$ line—indicated in Fig. 2 by grey shading.

The intensity distribution in the ribbon is, however, anisotropic. The edges of the ribbon are more intense than the center, reflecting the intensity distribution around the main FS (the DRs will necessarily have the same intensity distribution as the main FS). Finally, we point out the SFS, which follows the red lines underlying the map and is seen in these data more clearly than ever before.

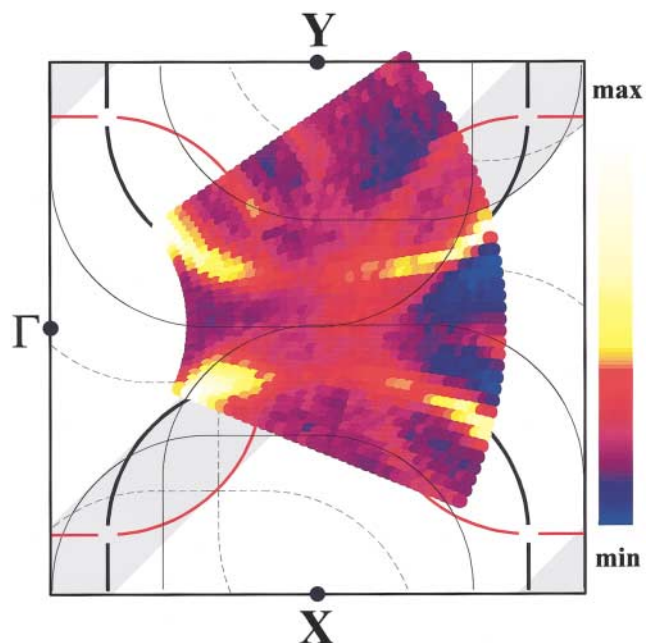


FIG. 2 (color). Normal state ($T = 120$ K) Fermi surface map of Bi2212. The color scale indicates the photoemission intensity at E_F [11]. The guidelines indicate the main FS (thick, black solid line); shadow FS (solid red line); first-order DRs (thin solid black line, on top of map), second-order DRs (dashed black line). For details see text.

The main point that is clear from Fig. 2 is the richness of structure in the ARPES data around \bar{M} . This arises from the complex interplay between main FS, DRs and the SFS features. As an example of this, one can see the overlap of the SFS and first-order DR features at about $0.6(\pi, \pi)$ as a bright spot on the map.

We emphasize that only an analysis of uninterpolated data recorded with high (E, \mathbf{k}) resolution on an extremely fine \mathbf{k} mesh can enable the discrimination between the numerous features concentrated within this small region of the Brillouin zone.

As a test of the robustness of the picture developed above, we show in Fig. 3 a large Fermi surface map of Pb-doped Bi2212. This time 3760 EDCs form the basis of the image. We chose the Pb-doped material as it does not possess the strong structural modulation along the crystallographic b direction which is characteristic of Bi2212 [12]. This should result, then, in the disappearance of DR-related features in the map.

As can be seen from Fig. 3, this is quite evidently the case as there is no intensity ribbon centered along the $(0, -\pi)$ - $(\pi, 0)$ line, and the intensity profile across the map is practically symmetrical about the Γ - \bar{M} - Z line. In this way we can put the assignment of the DR features in the Bi2212 data beyond any doubt.

The main FS, which is presented here with unprecedented clarity, has the form of tubes centered around the X, Y points. There are absolutely no indications of a Γ -centered, electronlike FS. The detailed topology of the main FS differs from that in the recent literature in a number of important points, which are related to the favorable experimental conditions used in this study.

First, the use of unpolarized radiation reduces the distorting effects of the photoemission matrix elements to a

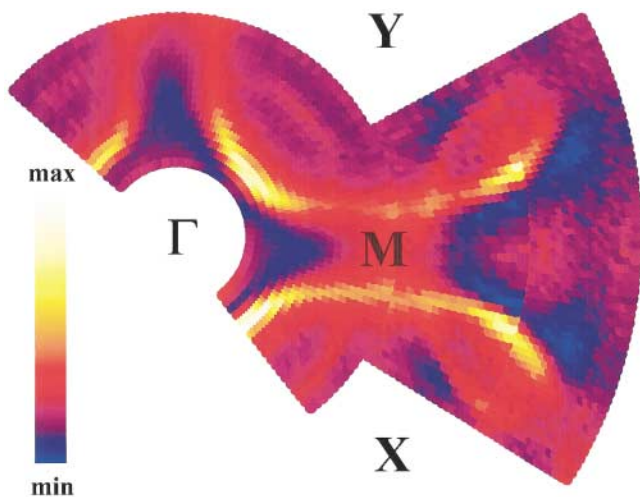


FIG. 3 (color). Normal state ($T = 120$ K) Fermi surface map of Pb-doped Bi2212. The color scale indicates the photoemission intensity at E_F [11]. The main FS has the topology of rounded tube sections and is holelike, centered upon the X, Y points. The shadow FS is also clearly visible. For details see text.

minimum—illustrated by the roughly equal intensity of the tube sections in both the ΓX and ΓY directions. All of the published FS investigations other than those of Aebi and co-workers [1] have used highly polarized synchrotron radiation and are therefore susceptible to extreme suppression of intensity in particular \mathbf{k} -space regions due purely to symmetry-related matrix element effects. In this way, mapping measurements using polarized radiation are inherently at a disadvantage when one wishes to determine the detailed FS topology without having to know, *a priori*, what it is. For example, Fermi surface maps of Bi2212 showed a strong dependence on the experimental geometry (and thus polarization conditions) [5,13]. Having made this point, it is obvious that maps recorded using polarized radiation cannot be used to support contentions [7] of an electronlike FS in Bi2212.

The second point concerns the exclusive use of *real* experimental data. If a coarse \mathbf{k} mesh is used to construct a map via interpolation, artifacts can result whereby the topology of the Fermi surface is extremely sensitive to the procedure used to define \mathbf{k}_F . As an illustration of this, we comment on the recent FS map of Feng *et al.* [8], derived from data recorded using polarized radiation at 51 \mathbf{k} -points in the $(0, 0)$ - (π, π) - $(0, \pi)$ octant of the Brillouin zone, which shows nested FS segments only when using the $\nabla n(\mathbf{k})$ method of determining \mathbf{k}_F [8]. The FS data presented here for both pristine and Pb-doped Bi2212 show a more curved FS arc in this region of \mathbf{k} -space, although a degree of parallelity across the \bar{M} point does exist. The important point here is that the FS topology in ARPES data sets of sufficient quality is extremely robust—the maps shown in Figs. 2 and 3 can be redrawn using either the I_{\max} or the $\nabla n(\mathbf{k})$ methods of determining \mathbf{k}_F , without altering the form of the main FS.

The third point in the comparative discussion of our data with that in the literature concerns the question of photon energy. We see no indication for an electronlike FS in either of the 2212 systems studied, neither from the He I data presented here nor from full FS maps of Pb-Bi2212 (not shown) recorded using unpolarized He II radiation ($h\nu = 40.8$ eV). We reach the same conclusion from the analysis of our synchrotron ARPES data from Bi2212 [14], in which no sign of a main band crossing is observed along $\Gamma\bar{M}$ for photon energies of either 40 or 50 eV (data not shown). If we use $h\nu = 32$ eV, we observe a strong suppression of the intensity of the saddle-point singularity states near \bar{M} . Since the Fermi surface of a material cannot depend on the photon energy used to measure it, it is clear that photon energies between 32–33 eV (as used in Refs. [5–8,13]) are not suited to giving an undistorted picture of the true FS of Bi2212.

Indeed, our data offer a natural explanation for the observations made with $h\nu = 32$ – 33 eV. The matrix-element mediated suppression of the saddle-point intensity for these photon energies explains both the suppression of spectral weight directly along the $(0, -\pi)$ - $(\pi, 0)$ line observed in

[5], and means that the edges of the ribbon mentioned earlier will become relatively more intense. Thus, traversal of the two edges of the ribbon feature could be mistakenly interpreted as a “main” band crossing along the Γ - \bar{M} line [7,8].

Finally, we turn to the shadow FS features. The most mundane explanation would be an extrinsic diffraction of the CuO_2 -plane photoelectrons on their way to or through the surface of the crystal, giving rise to full, tubelike copies of the main FS, i.e., the SFSs are mere DRs. Within this picture, as there is no evidence for reconstruction of the Sr-O or Bi-O layers of Bi2212 other than the well-known Bi-O modulation, the SFS features would then have to be *fifth-order* DRs [assuming \mathbf{q} is exactly $0.2(\pi, \pi)$, which is not the case]. For Bi2212 this scenario is clearly highly unrealistic, considering the relative intensities of the first- and second-order DR features seen in Figs. 1 and 2. In addition, if the SFS were a DR, it should show the same intensity distribution as the corresponding sections of the main FS (as is seen for the genuine Bi2212 DRs observed due to the Bi-O modulation). As this is not the case for the SFSs in either pristine or Pb-doped Bi2212, it would appear that they are intrinsic to the CuO_2 planes and are thus due to the presence of a Brillouin zone of half the size of the original. Such a reduction of the Brillouin zone could be due to structural effects, as has been illustrated for the case of Bi2201 [15]. However, there exists no evidence of this in the case of Bi2212.

Thus, at least for pristine Bi2212, all indicators point to a spin-related origin of the shadow FS in the photoemission data, as originally proposed [1,3]. Since there is electron diffraction evidence of a $c(2 \times 2)$ -like reconstruction in Pb-doped Bi2212 [12], no definitive conclusion is possible at this stage regarding the origin of the SFSs in this compound. Nevertheless, the strong similarities with regard to the topology and relative intensity of the shadow FSs in both the pristine and Pb-doped systems would seem to point to a common origin for these features.

Taking the SFSs to be intrinsic to the CuO_2 planes, regardless of their detailed origin, the overall FS topology cannot be that of the main FS tubes with additional SFS tubes shifted by (π, π) , as this would lead to a crossing of the two FS pieces (which is forbidden), as well as the necessity of accepting the simultaneous presence of hole-like and electronlike FSs of the same size originating from the same CuO_2 planes. Thus, the two FS pieces will be separated by a gap, whose magnitude depends on the interaction responsible for the Brillouin zone reduction. This gap could, however, be small enough to remain undetected in a photoemission experiment.

In conclusion, we have shown that high (E, \mathbf{k}) resolution and high \mathbf{k} -density angle-scanned photoemission data sets combining the advantages of both the mapping and EDC approaches give a self-consistent and robust picture of the nature and topology of the FS in the 2212-based materials. From a comparison of pristine and Pb-doped

Bi2212 we have shown there to be three different features in the ARPES data of Bi2212: (i) The main FS is hole-like, with the topology of a curved tube centered around the X, Y points; (ii) the Bi-O modulation gives rise to extrinsic diffraction replicas of the main FS which lead to high intensity ribbons centered on the $(0, -\pi)$ - $(\pi, 0)$ line; (iii) a shadow FS is also clearly present, which, at least in the case of Bi2212, is likely to be of spin-related origin.

We are grateful to the BMBF (05 SB8BDA 6), the DFG (Graduiertenkolleg “Struktur- und Korrelationseffekte in Festkörpern” der TU-Dresden), and the SMWK (4-7531.50-040-823-99/6) for financial support, and to U. Jännicke-Rössler and K. Nenkov for characterization of the crystals.

Note added.—While completing this paper, we became aware of a preprint [16] containing high k -density ARPES data of Bi2212 recorded using polarized radiation. These data, although measured deep in the superconducting state, are used to confirm the holelike nature of the main normal state FS and the distorting effect of matrix elements on the photoemission spectra when using $h\nu = 33$ eV.

*On leave from the Institute for Metal Physics, Kiev, Ukraine.

- [1] P. Aebi *et al.*, Phys. Rev. Lett. **72**, 2757 (1994).
- [2] See, e.g., H. Krakauer and W.E. Pickett, Phys. Rev. Lett. **60**, 1665 (1988).
- [3] A. P. Kampf and J.R. Schrieffer, Phys. Rev. B **42**, 7967 (1990).
- [4] H. Ding *et al.*, Phys. Rev. Lett. **76**, 1533 (1996).
- [5] N.L. Saini *et al.*, Phys. Rev. Lett. **79**, 3467 (1997).
- [6] N.L. Saini *et al.*, Phys. Rev. B **57**, R11 101 (1998).
- [7] Y.-D. Chuang *et al.*, Phys. Rev. Lett. **83**, 3717 (1999).
- [8] D.L. Feng *et al.*, cond-mat/9908056.
- [9] $X(Y)$ are the corners of the pseudotetragonal Brillouin zone, located at $2\pi/\mathbf{a}(\mathbf{b}) \approx 1.16 \text{ \AA}^{-1}$. \bar{M} is the midpoint of XY in the 2D Brillouin zone. We use the generally accepted shorthand: $\Gamma \equiv (0, 0)$, $X \equiv (\pi, -\pi)$, $Y \equiv (\pi, \pi)$, and $\bar{M} \equiv (\pi, 0)$.
- [10] G. Yang, J.S. Abell, and C.E. Gough, Appl. Phys. Lett. **75**, 1955 (1999).
- [11] Each EDC is normalized by division with the total integrated intensity of the spectrum. This gives a new criterion for determining \mathbf{k}_F , and can be viewed as a combination of the I_{\max} and $\nabla n(\mathbf{k})$ methods.
- [12] P. Schwaller *et al.*, J. Electron. Spectrosc. Relat. Phenom. **76**, 127 (1995).
- [13] A. Bianconi *et al.*, Physica (Amsterdam) **317C–318C**, 304 (1999).
- [14] Spectra were recorded at 100 K with $\Delta\Theta = \pm 1^\circ$ and $\Delta E = 70$ meV using linearly polarized synchrotron radiation from the U2-FSGM beam line at the BESSY I facility.
- [15] D. J. Singh and W.E. Pickett, Phys. Rev. B **51**, 3128 (1995).
- [16] H.M. Fretwell *et al.*, preceding Letter, Phys. Rev. Lett. **84**, 4449 (2000).